

RESEARCH ARTICLE

A synthesis method of spatial over-constrained mechanisms based on kinematics of serial manipulators

Fu-Hsiung Lee and Kuan-Lun Hsu* 

Department of Mechanical Engineering, National Taiwan University, Taipei, Taiwan, R.O.C.

*Corresponding author. E-mail: kuanlunhsu@ntu.edu.tw

Received: 13 December 2021; **Revised:** 4 April 2022; **Accepted:** 23 May 2022; **First published online:** 15 June 2022

Keywords: PPP open-chain manipulator, over-constrained mechanism, Euler Angles, mechanism topology, mechanism configuration

Abstract

This paper proposes a modular method based on the kinematics of serial manipulators to synthesize over-constrained mechanisms. Because the PPP manipulator has an unlimited work space, its end-effector can be constrained to trace a trajectory identical to those of another open-chain manipulator, including a P joint single link and an RR dyad. In doing so, two open-chain manipulators can be concatenated to form closed-loop mechanisms, including PPPP, PPPRR, or PPCR mechanisms. To design over-constrained mechanisms efficiently, the Denavit–Hartenberg convention is adopted to describe the PPP manipulator kinematically, and the Euler angles are utilized to derive geometric constraints of synthesized over-constrained mechanisms. Next, kinematic equations of the PPP manipulator can be modularized and applicable to analyze different closed-loop mechanisms. At last, by adjusting link lengths, twisted angles, and joint angles of the synthesized PPPRR and PPCR mechanisms to form other over-constrained mechanisms configurationally. The novelty of this research lies in modularizing the over-constrained mechanism into two movable serial manipulators whose end-effectors share identical trajectory and orientation. Thus, defining geometrical constraints of the over-constrained mechanism can be transformed into finding angular parameters describing the orientation of these two serial manipulators such that the end-effector coordinate system of two manipulators can properly be aligned. Angular parameters of the serial manipulators can be easily determined by means of Euler angles, which yields an advantage of easy calculation since it only involves the computation of Euler angles parameters. The presented method can be extended to the kinematic synthesis and analysis of more spatial closed-loop mechanisms.

1. Introduction

In mechanism and machine science, the degree of freedom of a mechanism has always been a far-reaching issue. Ahead of any analysis and synthesis, the most fundamental prerequisite is to confirm the existence of a mechanism by checking its degrees of freedom. In kinematics, Chebychev–Grübler–Kutzbach criterion [1, 2] is usually used to evaluate the degree of freedom of closed-loop linkages. Some closed-loop linkages have a degree of freedom less than one based on the Chebychev–Grübler–Kutzbach criterion, but they are mobile due to the unique geometric relationship of the mechanism. These mechanisms are called over-constrained mechanisms. Kinematicians have used different methods to discover many spatial mechanisms that violated the formula of degrees of freedom. Bennett [3] first proposed a four-bar linkage with the nonintersecting and nonparallel revolute joint in 1903. In 1922, Delassus used two revolute joints and prismatic joints to form a four-bar chain and derive the joint arrangements required to form a mobile linkage [4–6]. Afterward, Dimentberg [7] and Savage [8] also attempt to find geometric constraints of an overconstrained but mobile four-bar linkage with cylindrical joints. In 1967, Hunt investigated four-bar and five-bar linkages with prismatic joints and spherical joints and

restricted the rotational freedom of the ball joints to obtain a series of over-constrained mechanisms [9]. Waldron [10, 11] summed up geometric constraints of each joint in mobile four-bar linkages in space by solving kinematic closed-loop equations. In 1970, Pamidi and Soni [12, 13] fixed the cylindrical joints of a five-link mechanism to find out various five-link over-constrained mechanisms. Since the parallel revolute joints are the common geometric constraint addressed by Dimentberg, Savage, and Pamidi, Baker derived the possible combinations of the five-link mechanism by assuming that adjacent revolute joints are parallel [14, 15]. Research regarding over-constrained mechanisms has continued to evolve and develop in modern time. Lee and Hervé use the geometric relationship of the oblique circular cylinder to synthesize a set of five-link over-constraint mechanisms [16]. Guo et al. applied the screw theory to infer the characteristics and actual degrees of freedom of various multi-link over-constrained mechanisms [17]. However, some past literature searched for the geometric relationship of over-constrained mechanisms based on conjectures. For example, Pamidi and Soni first assumed that adjacent revolute joints of the five-link mechanism were parallel, and then derived the remaining geometric constraints through the closed-loop equations of the mechanism [12, 13]. For these related works, there are excessive assumptions and geometric restrictions for these four-bar or five-bar linkages. In addition, to find the existing criteria of an over-constrained mechanism, loop closure equations are required to relate link dimensions and joint variables. Derived loop closure equations are highly non-linear so that it is challenging to identify necessary geometrical constraints while maintaining the joint variables of the over-constrained architecture solvable. Therefore, an alternative method is proposed in this paper to examine the existence of over-constrained mechanisms. First, Section 2 investigated the forward and inverse kinematic analyses of a PPP open-chain manipulator. Next, Sections 2 and 3 present a synthesis method of several over-constrained mechanisms by constraining the end-effector of a PPP open-chain manipulator to a trajectory identical to those of another open-chain manipulator. Hence, angular parameters describing the orientation of one serial manipulator can be arbitrarily chosen. Next, by means of Euler's angle representation, angular parameters of another serial manipulator can then be easily determined such that the end-effector coordinate system of two manipulators can properly be aligned. Then, these two movable serial manipulators can be assembled to form an over-constrained architecture with mobility. Because of adopting the Euler angles parameters of the manipulator orientation, the geometric constraints of the five-link over-constrained mechanism obtained by the presented method will be less than that proposed by Pamidi and Soni [12, 13]. This presented approach also yields an advantage of easy calculation since it only involves the computation of Euler angles parameters.

Except for discovering over-constrained mechanisms from mathematical manipulations, Goldberg proposed combining two sets of Bennett four-bar linkages to form a new five-link over-constraining mechanism [18], thereafter Waldron [19], Baker [20], Chen [21], and others continued the same method to synthesize more over-constrained mechanisms. Although new mechanisms can be synthesized by synopating common portions of mating mechanisms, this approach has not yet made the best use of its strength because existing mechanisms are all based on a combination of Bennett four-bar linkages. Few kinematicians noticed the possibilities of new mechanisms that could be constructed by combining distinct source modules. Thus, Section 5 adopts the over-constrained mechanism obtained in Section 4 as source module, and then uses the configuration synthesis method proposed in the above-mentioned literature to further synthesize more prismatic joint-based over-constrained mechanisms.

2. Forward and inverse kinematic analyses of a PPP open-chain manipulator

In this paper, the Denavit–Hartenberg convention [22] is adopted to describe the three-link PPP manipulator kinematically. According to the coordinate system definition of D-H notation, the transformation matrix ${}^{i-1}T_i$ from the previous coordinate system $i - 1$ to the next coordinate system i can be expressed

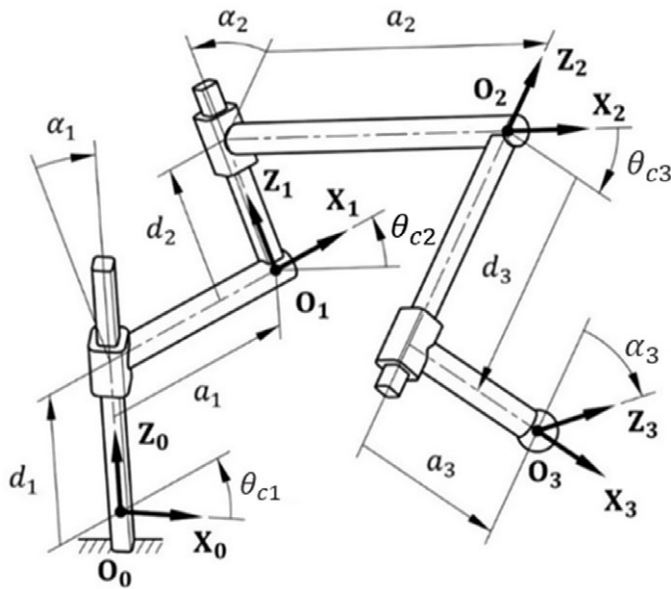


Figure 1. PPP open-chain manipulator.

as

$${}^{i-1}T_i = \begin{bmatrix} \cos \theta_i & -\sin \theta_i \cos \alpha_i & \sin \theta_i \sin \alpha_i & a_i \cos \theta_i \\ \sin \theta_i & \cos \theta_i \cos \alpha_i & -\cos \theta_i \sin \alpha_i & a_i \sin \theta_i \\ 0 & \sin \alpha_i & \cos \alpha_i & d_i \\ 0 & 0 & 0 & 1 \end{bmatrix} \tag{1}$$

After properly attaching frames $X_i Y_i Z_i$ ($i = 0, 1, 2,$ and 3) to each link of the PPP open-chain manipulator in Fig. 1, its D-H parameters can be tabulated in Table I. Notice that all joints are prismatic such that the parameter θ_i is constant and specifically denoted by θ_{ci} for distinction.

Substitute the D-H parameters of Table I into the transformation matrix ${}^{i-1}T_i$ in Eq. (1) and multiply the transformation matrices of three adjacent links to obtain the matrix 0_3T in Eq. (2). This matrix 0_3T represents the relative position and orientation relationship between the end-effector coordinate system $O_3 X_3 Y_3 Z_3$ and the fixed coordinate system $O_0 X_0 Y_0 Z_0$ of the PPP open-chain manipulator in Fig. 1.

$${}^0_3T = {}^0_1T {}^1_2T {}^2_3T \tag{2}$$

Matrix 0_3T contains a 3×3 rotation matrix 0_3R and a 3×1 translation matrix 0_3P , which can be expressed as

$${}^0_3T = \left[\begin{array}{ccc|c} & & & \\ & & & \\ & & & \\ \hline 0 & 0 & 0 & 1 \end{array} \right] \tag{3}$$

where the 3×3 rotation matrix 0_3R can be expressed as

$${}^0_3R = \begin{bmatrix} a_{11} & a_{12} & a_{13} \\ a_{21} & a_{22} & a_{23} \\ a_{31} & a_{32} & a_{33} \end{bmatrix} \tag{4}$$

Table I. Link parameters for the PPP open-chain manipulator.

Link	θ_i	d_i	a_i	α_i
1	θ_{c1}	d_1	a_1	α_1
2	θ_{c2}	d_2	a_2	α_2
3	θ_{c3}	d_3	a_3	α_3

The elements of the rotation matrix 0_3R in Eq. (4) can, respectively, be expressed as

$$a_{11} = c\theta_{c3}(c\theta_{c1}c\theta_{c2} - c\alpha_1s\theta_{c1}s\theta_{c2}) + s\theta_{c3}(-c\theta_{c2}c\alpha_1c\alpha_2s\theta_{c1} + s\alpha_1s\alpha_2s\theta_{c1} - c\theta_{c1}c\alpha_2s\theta_{c2}) \tag{5}$$

$$a_{12} = -c\alpha_3s\theta_{c3}(c\theta_{c1}c\theta_{c2} - c\alpha_1s\theta_{c1}s\theta_{c2}) + c\alpha_3c\theta_{c3}(-c\alpha_1c\alpha_2c\theta_{c2}s\theta_{c1} - c\alpha_2c\theta_{c1}s\theta_{c2} + s\theta_{c1}s\alpha_1s\alpha_2) + s\alpha_3(c\alpha_2s\theta_{c1}s\alpha_1 + c\alpha_1c\theta_{c2}s\theta_{c1}s\alpha_2 + c\theta_{c1}s\theta_{c2}s\alpha_2) \tag{6}$$

$$a_{13} = c\alpha_3(c\alpha_2s\theta_{c1}s\alpha_1 + c\alpha_1c\theta_{c2}s\theta_{c1}s\alpha_2 + c\theta_{c1}s\theta_{c2}s\alpha_2) + s\theta_{c3}s\alpha_3(c\theta_{c1}c\theta_{c2} - c\alpha_1s\theta_{c1}s\theta_{c2}) - c\theta_{c3}s\alpha_3(-c\alpha_1c\alpha_2c\theta_{c2}s\theta_{c1} - c\alpha_2c\theta_{c1}s\theta_{c2} + s\theta_{c1}s\alpha_1s\alpha_2) \tag{7}$$

$$a_{21} = c\theta_{c3}(c\alpha_1c\theta_{c1}s\theta_{c2} + c\theta_{c2}s\theta_{c1}) + s\theta_{c3}(c\alpha_1c\alpha_2c\theta_{c1}c\theta_{c2} - c\alpha_2s\theta_{c1}s\theta_{c1} - c\theta_{c1}s\alpha_1s\alpha_2) \tag{8}$$

$$a_{22} = -c\alpha_3s\theta_{c3}(c\alpha_1c\theta_{c1}s\theta_{c2} + c\theta_{c2}s\theta_{c1}) + c\alpha_3c\theta_{c3}(c\alpha_1c\alpha_2c\theta_{c1}c\theta_{c2} - c\alpha_2s\theta_{c1}s\theta_{c2} - c\theta_{c1}s\alpha_1s\alpha_2) + s\alpha_3(-c\alpha_2c\theta_{c1}s\alpha_1 - c\alpha_1c\theta_{c1}c\theta_{c2}s\alpha_2 + s\theta_{c1}s\theta_{c2}s\alpha_2) \tag{9}$$

$$a_{23} = c\alpha_3(-c\alpha_2c\theta_{c1}s\alpha_1 - c\alpha_1c\theta_{c1}c\theta_{c2}s\alpha_2 + s\theta_{c1}s\theta_{c2}s\alpha_2) + s\theta_{c3}s\alpha_3(c\alpha_1c\theta_{c1}s\theta_{c2} + c\theta_{c2}s\theta_{c1}) - c\theta_{c3}s\alpha_3(c\alpha_1c\alpha_2c\theta_{c1}c\theta_{c2} - c\alpha_2s\theta_{c1}s\theta_{c2} - c\theta_{c1}s\alpha_1s\alpha_2) \tag{10}$$

$$a_{31} = c\theta_{c3}s\theta_{c2}s\alpha_1 + s\theta_{c3}(c\alpha_2c\theta_{c2}s\alpha_1 + c\alpha_1s\alpha_2) \tag{11}$$

$$a_{32} = -c\alpha_3s\theta_{c2}s\theta_{c3}s\alpha_1 + c\alpha_3c\theta_{c3}(c\alpha_2c\theta_{c2}s\alpha_1 + c\alpha_1s\alpha_2) + s\alpha_3(c\alpha_1c\alpha_2 - c\theta_{c2}s\alpha_1s\alpha_2) \tag{12}$$

$$a_{33} = c\alpha_3(c\alpha_1c\alpha_2 - c\theta_{c2}s\alpha_1s\alpha_2) - c\theta_{c3}s\alpha_3(c\alpha_2c\theta_{c2}s\alpha_1 + c\alpha_1s\alpha_2) + s\theta_{c2}s\theta_{c3}s\alpha_1s\alpha_3 \tag{13}$$

Notice that in rotation matrix 0_3R there are only six angular parameters $\alpha_1, \alpha_2, \alpha_3, \theta_{c1}, \theta_{c2},$ and $\theta_{c3},$ which are all constant. In other words, the orientation of the end-effector of the PPP manipulator remains unchanged, while the input parameters of three prismatic joints $d_1, d_2,$ and d_3 are actuated.

In addition, the 3×1 matrix 0_3P in Eq. (3) can be expressed as

$${}^0_3P = \begin{bmatrix} c_1d_2 + c_2d_3 + c_3a_1 + c_4a_2 + c_5a_3 \\ c_6d_2 + c_7d_3 + c_8a_1 + c_9a_2 + c_{10}a_3 \\ d_1 + c_{11}d_2 + c_{12}d_3 + c_{13}a_2 + c_{14}a_3 \end{bmatrix} \tag{14}$$

where the coefficients of the translation matrix 0_3P in Eq. (14) can, respectively, be expressed as

$$c_1 = s\theta_{c1}s\alpha_1 \tag{15}$$

$$c_2 = c\alpha_2s\theta_{c1}s\alpha_1 + c\alpha_1c\theta_{c2}s\theta_{c1}s\alpha_2 + c\theta_{c1}s\theta_{c2}s\alpha_2 \tag{16}$$

$$c_3 = c\theta_{c1} \tag{17}$$

$$c_4 = c\theta_{c1}c\theta_{c2} - c\alpha_1s\theta_{c1}s\theta_{c2} \tag{18}$$

Table II. Link parameters for the three-link Cartesian robot.

Link	θ_i	d_i	a_i	α_i
1	0	d_1	0	-90°
2	90°	d_2	0	-90°
3	0	d_3	0	0

$$c_5 = c\theta_{c3}(c\theta_{c1}c\theta_{c2} - c\alpha_1s\theta_{c1}s\theta_{c2}) - s\theta_{c3}(c\alpha_1c\alpha_2c\theta_{c2}s\theta_{c1} + c\alpha_2c\theta_{c1}s\theta_{c2} - s\theta_{c1}s\alpha_1s\alpha_2) \tag{19}$$

$$c_6 = -c\theta_{c1}s\alpha_1 \tag{20}$$

$$c_7 = -c\alpha_2c\theta_{c1}s\alpha_1 - c\alpha_1c\theta_{c1}c\theta_{c2}s\alpha_2 + s\theta_{c1}s\theta_{c2}s\alpha_2 \tag{21}$$

$$c_8 = s\theta_{c1} \tag{22}$$

$$c_9 = c\alpha_1c\theta_{c1}s\theta_{c2} + c\theta_{c2}s\theta_{c1} \tag{23}$$

$$c_{10} = c\theta_{c3}(c\alpha_1c\theta_{c1}s\theta_{c2} + c\theta_{c2}s\theta_{c1}) + s\theta_{c3}(c\alpha_1c\alpha_2c\theta_{c1}c\theta_{c2} - c\alpha_2s\theta_{c1}s\theta_{c2} - c\theta_{c1}s\alpha_1s\alpha_2) \tag{24}$$

$$c_{11} = c\alpha_1 \tag{25}$$

$$c_{12} = c\alpha_1c\alpha_2 - c\theta_{c2}s\alpha_1s\alpha_2 \tag{26}$$

$$c_{13} = s\theta_{c2}s\alpha_1 \tag{27}$$

$$c_{14} = c\theta_{c3}s\theta_{c2}s\alpha_1 + s\theta_{c3}(c\alpha_2c\theta_{c2}s\alpha_1 + c\alpha_1s\alpha_2) \tag{28}$$

From Eq. (14), it is known that the three elements of the translation matrix 0_3P have a linear relationship with three prismatic joints d_1 , d_2 , and d_3 . Suppose that the ranges of three prismatic joints d_1 , d_2 , and d_3 are infinite. Thus, the origin of the end-effector coordinate system O_3 has no boundary workspace. In other words, the end-effector of the PPP manipulator can be moved to any point in the three-dimensional space theoretically.

If the three sliding joint axes are arranged to be perpendicular to each other, as described by the D-H parameters tabulated in Table II. By substituting these D-H parameters into homogeneous transformation matrices, a relatively simple expression for the elements can be obtained as expressed in Eq. (29):

$${}^0_3T = \begin{bmatrix} 0 & 0 & -1 & -d_3 \\ 0 & -1 & 0 & d_2 \\ -1 & 0 & 0 & d_1 \\ 0 & 0 & 0 & 1 \end{bmatrix} \tag{29}$$

Suppose that the endpoint of this manipulator, relative to the end-effector coordinate system and the fixed coordinate system, is expressed as $[x, y, z]^T$ and $[X, Y, Z]^T$, respectively. Coordinates $[x, y, z]^T$ and $[X, Y, Z]^T$ can be related by the following coordinate transformation:

$$\begin{bmatrix} X \\ Y \\ Z \\ 1 \end{bmatrix} = {}^0_3T \begin{bmatrix} x \\ y \\ z \\ 1 \end{bmatrix} \tag{30}$$

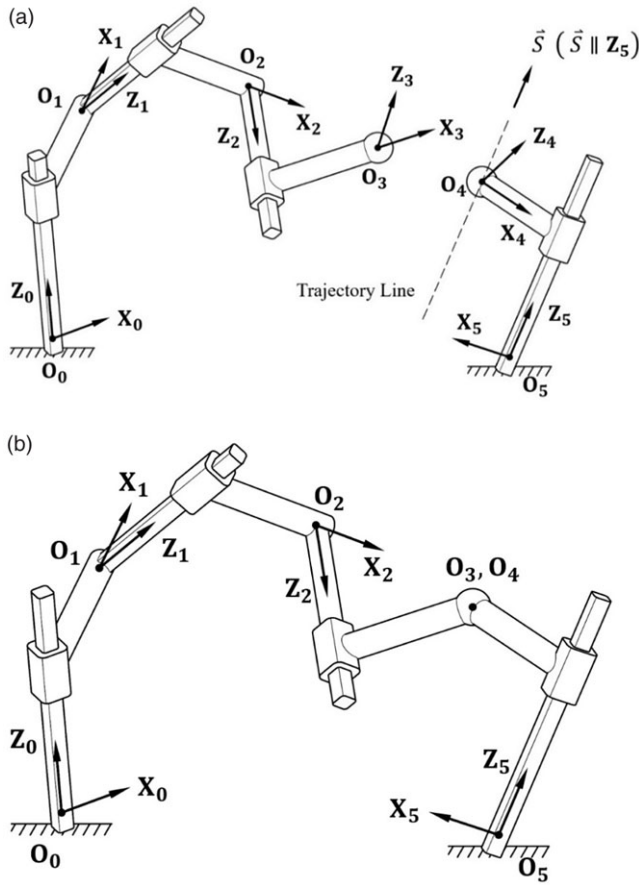


Figure 2. Spatial PPPP mechanism by combining two open-chain manipulators.

Hence, expanding Eq. (30) yields

$$\begin{bmatrix} X \\ Y \\ Z \\ 1 \end{bmatrix} = \begin{bmatrix} -d_3 - z \\ d_2 - y \\ d_1 - x \\ 1 \end{bmatrix} \tag{31}$$

From Eq. (31), it can be found that the end-point of the manipulator is controlled by three joint variables d_1 , d_2 , and d_3 . From Eq. (29), we found that this manipulator can be configured into a Cartesian robot, which has linear movements in the three Cartesian coordinates, that is, in x , y , and z axes that are mutually perpendicular.

3. Synthesis of a spatial PPPP mechanism

In Section 2, it has been demonstrated that the three-link PPP manipulator has a fixed orientation and an unlimited workspace. Therefore, its end-effector can be constrained to trace a trajectory identical to that of another open-chain manipulator. If another open-chain manipulator is a single link adjacent to the fixed link by a prismatic joint in Fig. 2(a), the PPP manipulator and the single link can be concatenated to form a spatial closed-loop PPPP mechanism in Fig. 2(b).

When such a closed-loop chain containing four prismatic joints is formed, the multiplication of transformation matrices between adjacent links of such a closed-loop chain is equal to an identity matrix, namely,

$${}^0T_2^1T_3^2T_4^3T = I_4 \tag{32}$$

To find geometric constraints of twisted angles between the links, a 3×3 rotation matrix ${}^{i-1}R_i$ is extracted from Eq. (32) and a closed-loop equation can then be expressed as

$${}^0R_2^1R_3^2R_4^3R = I_3 \tag{33}$$

To avoid the complexity faced by Pamidi and Soni [12, 13], this paper proposes an alternative way to simplify the solutions of the closed-loop equation. First, multiply Eq. (33) by an inverse matrix ${}^3R_4^{-1}$ to obtain the following equation, namely,

$${}^0R_2^1R_3^2RR = {}^3R^{-1} \tag{34}$$

From the perspective of kinematics, rotation matrix ${}^0R_2^1R_3^2R$ represents the end-effector orientation of the PPP manipulator relative to the fixed coordinate system. Similarly, rotation matrix ${}^3R^{-1}$ represents the end-effector orientation of the P-joint single-arm manipulator relative to the fixed coordinate system. Therefore, Eq. (34) implies that when the PPPP mechanism satisfies the closed-loop equation, the end-effector orientation of the PPP manipulator and the P-joint single-arm manipulator must be identical. Therefore, this paper attempts to meet the closed-loop equation of the PPPP mechanism by exploring the end-effector orientation of the PPP manipulator. To this end, rotation matrix ${}^0R_2^1R_3^2R = {}^0R_3$ of the PPP manipulator is set to be equal to Euler angle representation $R_{Euler}(\alpha, \beta, \gamma)$, as shown in Appendix A, namely,

$${}^0R_3 = R_{Euler}(\alpha, \beta, \gamma) \tag{35}$$

Eq. (35) can further be rearranged as

$${}^0RR^{-1}{}_{Euler}(\alpha, \beta, \gamma) = I_3 \tag{36}$$

From Eq. (36), multiplying rotation matrix 0R_3 and $R_{Euler}^{-1}(\alpha, \beta, \gamma)$ together forms an identity matrix I_3 . This constraint in the Equation can be regarded as the necessary condition to meet the closed-loop equation of the PPPP mechanism. In addition, once Euler angle parameters (α, β, γ) are determined and used to characterize the P-joint single-arm manipulator, the closed-loop equation of the PPPP mechanism can be met satisfactorily. However, the P-joint single-arm manipulator only requires two angular parameters according to the D-H notation. To properly substitute Euler angle parameters into the D-H parameters, this paper proposes decomposing the Euler angles convention such that Euler angle parameters (α, β, γ) can be appropriately fit into the D-H notation.

Two types of Euler angles notations, ZXX and XZX, are used for demonstration.

First, suppose that rotation matrix ${}^0R_2^1R_3^2R$ of the PPP manipulator is represented by the ZXX Euler angles, which is

$${}^0R_2^1R_3^2R = R_z(\gamma) R_x(\beta) R_z(\alpha) \tag{37}$$

Eq. (37) is deliberately rearranged as

$$R_z^{-1}(\gamma) {}^0R_2^1R_3^2R = R_x(\beta) R_z(\alpha) \tag{38}$$

such that the right side of the equal sign only contains matrix $R_x(\beta)$ and $R_z(\alpha)$. In doing so, only two Euler angle parameters α and β are required and thus can be fit into the D-H notation for describing the P-joint single-arm manipulator.

Next, matrix 0R_3 in Eq. (38) is further decomposed into a multiplication of matrices $R_z(\theta_{c1})$ and $R_x(\alpha_1)$, namely,

$$R_z^{-1}(\gamma) R_z(\theta_{c1}) R_x(\alpha_1) {}^0R_2^1R_3^2R = R_x(\beta) R_z(\alpha) \tag{39}$$

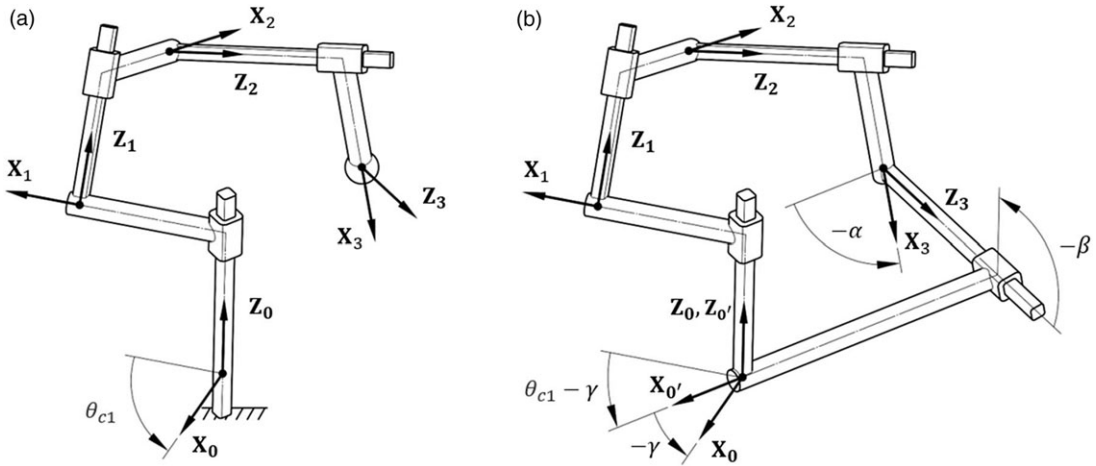


Figure 3. Synthesis of spatial PPPR mechanism using ZXZ Euler angles convention.

In Eq. (39), matrix $R_z^{-1}(\gamma)$ and $R_z(\theta_{c1})$ can be combined as one rotation of $\theta_{c1} - \gamma$ around the z-axis, namely,

$$R_z(\theta_{c1} - \gamma) R_x(\alpha_1) {}^1_2R_3^2R = R_x(\beta) R_z(\alpha) \tag{40}$$

Let $R_z(\theta_{c1} - \gamma) R_x(\alpha_1)$ and $R_x(\beta) R_z(\alpha)$ be denoted by one matrix 0_1R and ${}^3_4R^{-1}$, respectively, such that Euler angle parameters can be appropriately fit into the D-H notation and the successively rotational transformations along the closed-loop PPPP mechanism can be expressed as

$${}^0_1R {}^1_2R {}^2_3R = {}^3_4R^{-1} \tag{41}$$

The ZXZ Euler angles embedded in Eq. (41) can be interpreted using Fig. 3 from the perspective of kinematics. Fig. 3(a) illustrates an open-loop PPP manipulator whose end-effector and initial coordinate system are $O_3X_3Y_3Z_3$ and $O_0X_0Y_0Z_0$, respectively. If a P-joint single-arm manipulator is connected to the open-loop PPP manipulator to form a closed-loop mechanism, the P-joint single-arm manipulator must share identical end-effector and initial coordinate system $O_3X_3Y_3Z_3$ and $O_0X_0Y_0Z_0$. For this purpose, as shown in Fig. 3(b), angular parameters of the P-joint single-arm manipulator can be substituted with Euler angle parameters (α, β, γ) so that end-effector coordinate system $O_3X_3Y_3Z_3$ can be transformed to initial coordinate system $O_0X_0Y_0Z_0$ via the newly added single-arm manipulator. Besides, from Fig. 3(b), it can be interpreted that matrix ${}^3_4R^{-1}$ represents a coordinate system transformation from $O_3X_3Y_3Z_3$ to $O_0'X_0'Y_0'Z_0'$, and matrix 0_1R represents a coordinate system transformation from $O_1X_1Y_1Z_1$ to $O_0'X_0'Y_0'Z_0'$.

Because Euler angle γ can be used to orientate $X_{0'}$ toward X_0 , θ_{c1} in Eq. (40) can be assumed as a dummy parameter equal to zero. At last, D-H parameters in Eq. (41) can be tabulated in Table III.

Now, suppose that rotation matrix ${}^0_1R {}^1_2R {}^2_3R$ of the PPP manipulator is represented by the ZXZ Euler angles, which is

$${}^0_1R {}^1_2R {}^2_3R = R_x(\gamma) R_z(\beta) R_x(\alpha) \tag{42}$$

Eq. (42) is deliberately rearranged as

$${}^0_1R {}^1_2R {}^2_3R R_x^{-1}(\alpha) = R_x(\gamma) R_z(\beta) \tag{43}$$

such that the right side of the equal sign only contains matrix $R_x(\gamma)$ and $R_z(\beta)$. In doing so, only two Euler angle parameters γ and β are required and thus can be fit into D-H notation for describing the P-joint single-arm manipulator.

Table III. Link parameters involving ZXZ Euler angles convention for the closed-loop PPPP mechanism.

Link	θ_i	d_i	a_i	α_i
1	$-\gamma$	d_1	a_1	α_1
2	θ_{c2}	d_2	a_2	α_2
3	θ_{c3}	d_3	a_3	α_3
4	$-\alpha$	d_4	a_4	$-\beta$

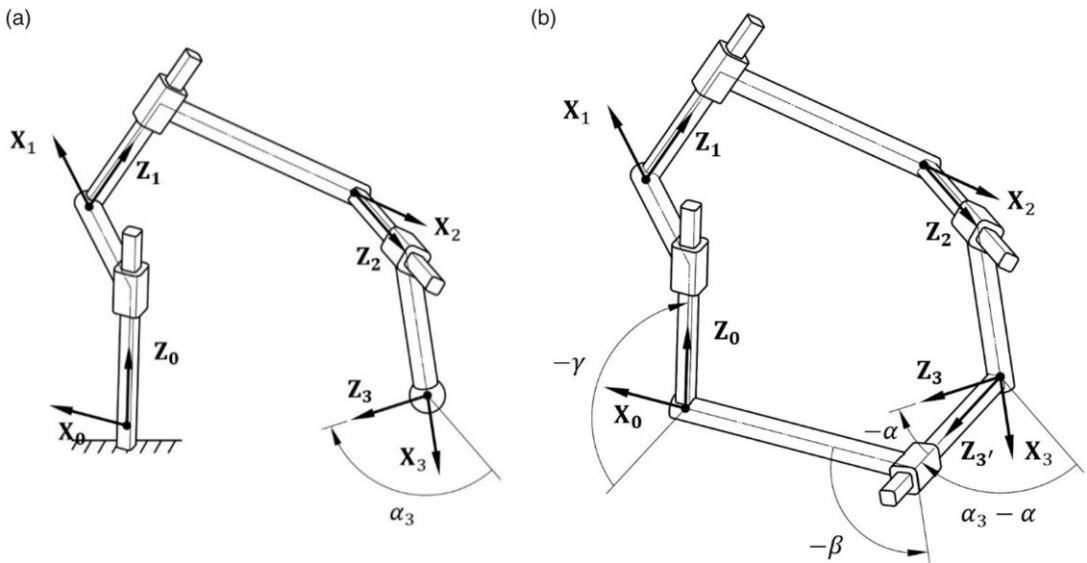


Figure 4. Synthesis of spatial PPPP mechanism using XZX Euler Angles convention.

Next, matrix 3_1R in Eq. (43) is further decomposed into a multiplication of matrices $R_z(\theta_{c3})$ and $R_x(\alpha_3)$, namely,

$${}^0_1R_2RR_z(\theta_{c3})R_x(\alpha_3)R_x^{-1}(\alpha) = R_x(\gamma)R_z(\beta) \tag{44}$$

In Eq. (44), matrix $R_x(\alpha_3)$ and $R_x^{-1}(\alpha)$ can be combined as one rotation of $\alpha_3 - \alpha$ around the z-axis, namely,

$${}^0_1R_2RR_z(\theta_3)R_x(\alpha_3 - \alpha) = R_x(\gamma)R_z(\beta) \tag{45}$$

Let $R_z(\theta_3)R_x(\alpha_3 - \alpha)$ and $R_x(\gamma)R_z(\beta)$ be denoted by one matrix 2_3R and ${}^4_4R^{-1}$, respectively, such that Euler angle parameters can be appropriately fit into the D-H notation and the successively rotational transformations along the closed-loop PPPP mechanism can be expressed as

$${}^0_1R_2R_3^2R = {}^4_4R^{-1} \tag{46}$$

The XZX Euler angles embedded in Eq. (46) can be interpreted using Fig. 4 from the perspective of kinematics. Fig. 4(a) illustrates an open-loop PPP manipulator whose end-effector and initial coordinate system are $O_3X_3Y_3Z_3$ and $O_0X_0Y_0Z_0$, respectively. If a P-joint single-arm manipulator is connected to the open-loop PPP manipulator to form a closed-loop mechanism, the P-joint single-arm manipulator must share identical end-effector and initial coordinate system $O_3X_3Y_3Z_3$ and $O_0X_0Y_0Z_0$. For this purpose, as shown in Fig. 4(b), angular parameters of the P-joint single-arm manipulator can be substituted with Euler angle parameters (α, β, γ) so that end-effector coordinate system $O_3X_3Y_3Z_3$ can be transformed to initial coordinate system $O_0X_0Y_0Z_0$ via the newly added single-arm manipulator. Besides,

Table IV. Link parameters involving XZX Euler angles convention for the closed-loop PPPP mechanism.

Link	θ_i	d_i	a_i	α_i
1	θ_{c1}	d_1	a_1	α_1
2	θ_{c2}	d_2	a_2	α_2
3	θ_{c3}	d_3	a_3	$-\alpha$
4	$-\beta$	d_4	a_4	$-\gamma$

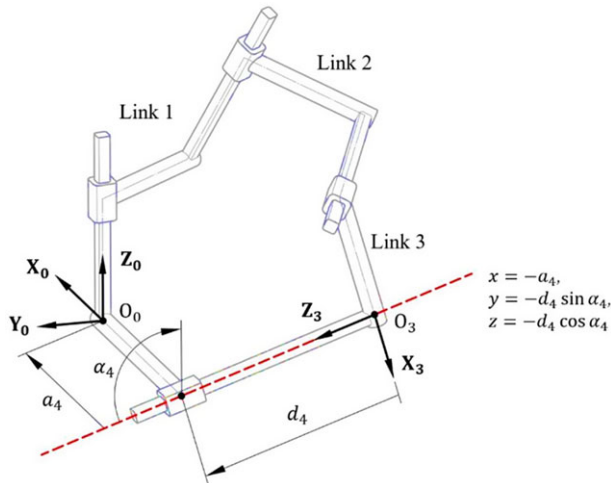


Figure 5. Kinematic analysis of a spatial PPPP mechanism.

from Fig. 4(b), it can be interpreted that matrix ${}^3_4R^{-1}$ represents a coordinate system transformation from $O_3'X_3'Y_3'Z_3'$ to $O_0'X_0'Y_0'Z_0'$ and matrix 2_3R represents a coordinate system transformation from $O_3'X_3'Y_3'Z_3'$ to $O_2X_2Y_2Z_2$.

Because Euler angle α can be used to orientate Z_3 toward Z_3' , α_3 in Eq. (45) can be assumed as a dummy parameter equal to zero. At last, D-H parameters in Equation can be tabulated in Table IV.

Because the motion of the PPPP mechanism can be characterized by picturing its end-effector being constrained to trace a linear trajectory, the kinematics of the PPPP mechanism can be analyzed based on the kinematics of the PPP manipulator. In reference to Fig. 5, the end-effector and initial coordinate system of the PPP manipulator are denoted as $O_3X_3Y_3Z_3$ and $O_0X_0Y_0Z_0$, respectively. When the PPPP mechanism is moving, the origin O_3 of the end-effector is constrained to move along axis Z_3 , a straight line whose equation can be expressed as

$$L(d_4) = \begin{bmatrix} -a_4 \\ -d_4 \sin \alpha_4 \\ -d_4 \cos \alpha_4 \end{bmatrix} \tag{47}$$

By setting the elements of the 3×1 matrix 0_3P , as expressed in Eq. (14), equal to these of $L(d_4)$ in Eq. (47), joints variables d_1 , d_2 , and d_3 can be expressed in terms of d_4 , namely,

$$d_1 = -(a_2 + a_1c\theta_{c2} + a_3c\theta_{c3} + a_4c\theta_{c1}c\theta_{c2} + d_4\alpha_4s\alpha_1s\theta_{c2} + d_4s\alpha_4c\theta_{c2}s\theta_{c1} - a_4\alpha_1s\theta_{c1}s\theta_{c2} + d_4\alpha_1s\alpha_4c\theta_{c1}s\theta_{c2}) / s\alpha_1s\theta_{c2} \tag{48}$$

Table V. ZYZ Euler angles convention for synthesized PPPP mechanism.

Link	θ_i	d_i	a_i	α_i
1	$-\gamma$	d_1	130	45°
2	-70°	d_2	140	55°
3	-60°	d_3	160	70°
4	$-\alpha$	d_4	160	$-\beta$

Table VI. D-H table for synthesized PPPP mechanism.

Link	θ_i	d_i	a_i	α_i
1	-55.7477°	d_1	130	45°
2	-70°	d_2	140	55°
3	-60°	d_3	160	70°
4	-97.2240°	d_4	160	74.0753°

$$\begin{aligned}
 d_2 = & (c\alpha_2 s\alpha_1 c\theta_{c1} - s\alpha_2 s\theta_{c1} s\theta_{c2} + c\alpha_1 s\alpha_2 c\theta_{c1} c\theta_{c2}) (a_4 + a_1 c\theta_{c1} + a_2 c\theta_{c1} c\theta_{c2} + a_3 c\theta_{c1} c\theta_{c2} c\theta_{c3} \\
 & - a_2 c\alpha_1 s\theta_{c1} s\theta_{c2} - a_3 c\alpha_1 c\theta_{c3} s\theta_{c1} s\theta_{c2} - a_3 c\alpha_2 c\theta_{c1} s\theta_{c2} s\theta_{c3} + a_3 s\alpha_1 s\alpha_2 s\theta_{c1} s\theta_{c3} \\
 & - a_3 c\alpha_1 c\alpha_2 c\theta_{c2} s\theta_{c1} s\theta_{c3}) / (s\alpha_1 s\alpha_2 s\theta_{c2} + (c\alpha_2 s\alpha_1 s\theta_{c1} + s\alpha_2 c\theta_{c1} s\theta_{c2} + c\alpha_1 s\alpha_2 c\theta_{c2} s\theta_{c1}) (d_4 s\alpha_4 \\
 & + a_1 s\theta_{c1} + a_3 c\theta_{c3} (c\theta_{c2} s\theta_{c1} + c\alpha_1 c\theta_{c1} s\theta_{c2})) - a_3 s\theta_{c3} (s\alpha_1 s\alpha_2 c\theta_{c1} + c\alpha_2 s\theta_{c1} s\theta_{c2} - c\alpha_1 c\alpha_2 c\theta_{c1} c\theta_{c2}) \\
 & + a_2 c\theta_{c2} s\theta_{c1} + a_2 c\alpha_1 c\theta_{c1} s\theta_{c2})) / s\alpha_1 s\alpha_2 s\theta_{c2} \tag{49}
 \end{aligned}$$

$$d_3 = - (a_1 + a_2 c\theta_{c2} + a_4 c\theta_{c1} + a_3 c\theta_{c2} c\theta_{c3} + d_4 s\alpha_4 s\theta_{c1} - a_3 c\alpha_2 s\theta_{c2} s\theta_{c3}) / s\alpha_2 s\theta_2 \tag{50}$$

A numerical example is provided to illustrate using the ZYZ Euler angles convention to synthesize an over-constrained PPPP mechanism. First, five arbitrary angular parameters $\{\theta_{c2}, \theta_{c3}, \alpha_1, \alpha_2, \alpha_3\} = \{-70^\circ, -60^\circ, 45^\circ, 55^\circ, 70^\circ\}$ and four-link parameters $\{a_1, a_2, a_3, a_4\} = \{130, 140, 160, 160\}$ are assumed and substituted into Table III, which is tabulated in Table V.

Next, substituting five arbitrary angular parameters $\{\theta_{c2}, \theta_{c3}, \alpha_1, \alpha_2, \alpha_3\} = \{-70^\circ, -60^\circ, 45^\circ, 55^\circ, 70^\circ\}$ and $\theta_{c1} = 0$ into rotation matrix 0_3R in Eq. (4) yields,

$${}^0_3R(\theta_{c1} = 0, \theta_{c2}, \theta_{c3}, \alpha_1, \alpha_2, \alpha_3) = \begin{bmatrix} a_{11} & a_{12} & a_{13} \\ a_{21} & a_{22} & a_{23} \\ a_{31} & a_{32} & a_{33} \end{bmatrix} \tag{51}$$

Then, use to calculate Euler angle β , which is

$$\beta = \pm \cos^{-1} a_{33} = \pm 87.273^\circ \tag{52}$$

Here, the negative value of Euler angle β is adopted to solve for Euler angle α and γ using Eqs. (A4) and (A5), which are

$$\alpha = \text{atan2}(-a_{31}, -a_{32}) = 97.2240^\circ \tag{53}$$

$$\gamma = \text{atan2}(-a_{13}, a_{23}) = 55.7477^\circ \tag{54}$$

The aforementioned results, which are tabulated in Table VI, can be used to structure a closed-loop PPPP mechanism, as shown in Fig. 6.

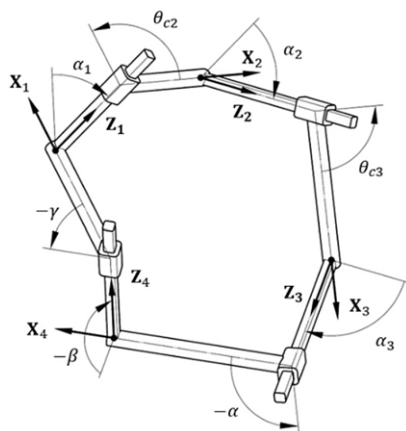


Figure 6. Synthesized PPPP mechanism using presented methodology.

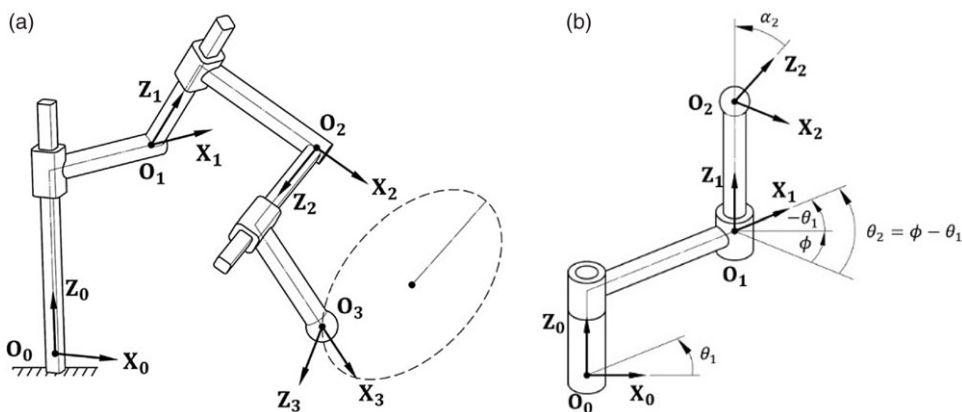


Figure 7. Two open-chain manipulators used to form a spatial PPPRR mechanism.

4. Synthesis of a spatial over-constrained five-bar mechanisms and their isomers PPPRR mechanism

4.1. PPPRR mechanism

Because the end-effector of the PPP manipulator can be constrained to move along an arbitrary space curve, in Section 3, its trajectory is purposely assigned to move along a straight line and connected to a P-joint single-arm manipulator to form a closed-loop PPPP mechanism. This synthesis concept is further extended by assigning the end-effector trajectory of the PPP manipulator to be circular, as shown in Fig. 7(a). Hence, the end-effector now can be connected to a two-arm RR manipulator, as shown in Fig. 7(b).

Recall that the orientation of the PPP manipulator is fixed. To form a closed-loop mechanism by combining a PPP manipulator with a RR manipulator, the end-effector of the RR manipulator must be constrained to move along a circle without changing its orientation. In reference to Fig. 7(b), when joint axes of two revolute joints are parallel and the second joint variable θ_2 is a summation of adding the first joint variable θ_1 with an arbitrary constant ϕ , endpoint O_2 of the RR manipulator traces a circular trajectory and the orientation of the end-effector coordinate system $O_2X_2Y_2Z_2$ is always identical to that of $O_0X_0Y_0Z_0$. Hence, the RR manipulator can be combined with the PPP manipulator by sharing the same end-effector trajectory and orientation.

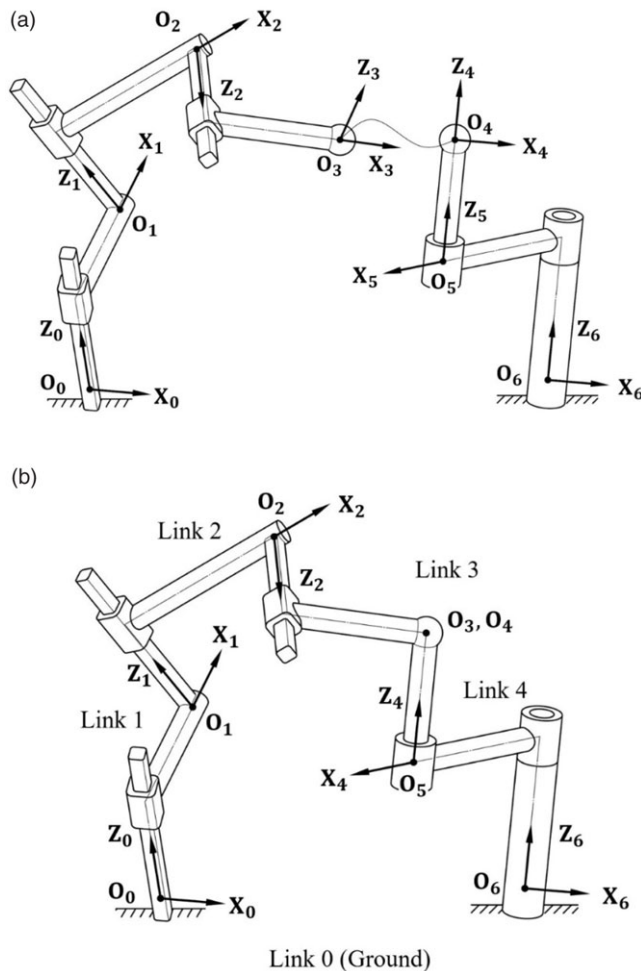


Figure 8. Spatial PPPRR mechanism by combining two open-chain manipulators.

For a better illustration, coordinate systems of the PPP and RR manipulator defined according to the D-H notation are labeled in Fig. 8(a). $O_3X_3Y_3Z_3$ and $O_0X_0Y_0Z_0$ are the end-effector and initial coordinate systems, respectively, for the PPP manipulator. $O_4X_4Y_4Z_4$ and $O_6X_6Y_6Z_6$ are the end-effector and initial coordinate systems, respectively, for the RR manipulator. Notice that revolute joint Z_4 is parallel to revolute joint Z_5 . Now, let origin O_3 be coincident with origin O_4 and the orientation of coordinate system $O_3X_3Y_3Z_3$ remain unchanged relative to that of $O_4X_4Y_4Z_4$. In doing so, a closed-loop five-bar PPPRR mechanism is formed, as shown in Fig. 8(b).

The DH parameters for the PPPRR mechanism are presented in Table VII. Notice that all joint variables θ_i for prismatic pairs are specifically denoted by a constant θ_{ci} for distinction. Likewise, all joint offsets d_i for revolute pairs are specifically denoted by a constant d_{ci} for distinction. In addition, to form a closed-loop mechanism by combining a PPP and RR manipulator, two revolute joint axes of the RR manipulator must be parallel and the difference of their joint variables must be constant. Thus, two more constraints that must be met can be expressed as

$$\alpha_4 = 0 \tag{55}$$

$$\theta_5 = \phi - \theta_4 \tag{56}$$

Table VII. Link parameters for the closed-loop PPPRR mechanism.

Link	θ_i	d_i	a_i	α_i
1	θ_{c1}	d_1	a_1	α_1
2	θ_{c2}	d_2	a_2	α_2
3	θ_{c3}	d_3	a_3	α_3
4	θ_4	d_{c4}	a_4	α_4
5	θ_5	d_{c5}	a_4	α_5

Next, by substituting the D-H parameters in Table VII into the transformation matrix of the PPPRR mechanism, a multiplication of five 3×3 rotation matrices can be extracted and expressed as

$${}^0R_2^1R_3^2R_4^3R_5^4R = I_3 \tag{57}$$

Multiply Eq. (57) by inverse matrices ${}^4R^{-1}{}^3R^{-1}$ to obtain the following equation, namely,

$${}^0R_2^1R_3^2R = {}^4R^{-1}{}^3R^{-1} \tag{58}$$

Substituting Eqs. (55) and (56) into matrices ${}^4R^{-1}{}^3R^{-1}$ yields the following equation:

$${}^4R^{-1}{}^3R^{-1} = \begin{bmatrix} c\phi & s\phi & 0 \\ -s\phi c\alpha_5 & c\phi c\alpha_5 & s\alpha_5 \\ s\phi s\alpha_5 & -c\phi s\alpha_5 & c\alpha_5 \end{bmatrix} \tag{59}$$

It can be found that ${}^4R^{-1}{}^3R^{-1}$ in Eq. (59) can be further decomposed into a multiplication of matrices $R_x(-\alpha_5)$ and $R_z(-\phi)$, namely,

$$R_x(-\alpha_5)R_z(-\phi) = \begin{bmatrix} 1 & 0 & 0 \\ 0 & c\alpha_5 & s\alpha_5 \\ 0 & -s\alpha_5 & c\alpha_5 \end{bmatrix} \begin{bmatrix} c\phi & s\phi & 0 \\ -s\phi & c\phi & 0 \\ 0 & 0 & 1 \end{bmatrix} \tag{60}$$

Therefore, from Eqs. (58), (59), and (60), we can find that

$${}^0R_2^1R_3^2R = R_x(-\alpha_5)R_z(-\phi) \tag{61}$$

Now, a similar manipulation of rotation matrices, as mentioned in the previous section, can be applied to properly fit Euler angle parameters into D-H parameters. Two types of Euler angles notations, ZXZ and XZX, are used for demonstration. First, we discuss the case using the ZXZ Euler angles. In reference to Eq. (40), this equation is deliberately rearranged as

$${}^0R_2^1R_3^2R = R_x(\beta)R_z(\alpha) \tag{62}$$

where,

$${}^0R = R_z(\theta_{c1} - \gamma)R_x(\alpha_1) \tag{63}$$

By comparing Eq. (61) with (62), it can be found that the ZXZ Euler angle parameters (α, β, γ) can be appropriately fit into the D-H parameters in Table VIII describing the closed-loop equation of the PPPRR mechanism.

Next, we discuss the case using the XZX Euler angles. In reference to Eq. (45), this equation is deliberately rearranged as

$${}^0R_2^1R_3^2R = R_x(\gamma)R_z(\beta) \tag{64}$$

where,

$${}^2R = R_z(\theta_3)R_x(\alpha_3 - \alpha) \tag{65}$$

Table VIII. Link parameters involving ZXZ Euler angles convention for the closed-loop PPPRR mechanism.

Link	θ_i	d_i	a_i	α_i
1	$-\gamma$	d_1	a_1	α_1
2	θ_{c2}	d_2	a_2	α_2
3	θ_{c3}	d_3	a_3	α_3
4	θ_4	d_{c4}	a_4	0
5	$-\alpha - \theta_4$	d_{c5}	a_5	$-\beta$

Table IX. Link parameters involving XZX Euler angles convention for the closed-loop PPPRR mechanism.

Link	θ_i	d_i	a_i	α_i
1	θ_{c1}	d_1	a_1	α_1
2	θ_{c2}	d_2	a_2	α_2
3	θ_{c3}	d_3	a_3	$-\alpha$
4	θ_4	d_{c4}	a_4	0
5	$-\beta - \theta_4$	d_{c5}	a_5	$-\gamma$

Table X. ZXZ Euler angles convention for synthesized PPPRR mechanism.

Link	θ_i	d_i	a_i	α_i
1	$-\gamma$	d_1	180	50°
2	-60°	d_2	140	40°
3	-70°	d_3	130	55°
4	θ_4	85	100	0
5	θ_5	55	120	$-\beta$

By comparing Eq. (61) with (64), it can be found that the XZX Euler angle parameters (α, β, γ) can be appropriately fit into the D-H parameters in Table IX describing the closed-loop equation of the PPPRR mechanism.

A numerical example is provided to illustrate using the ZXZ Euler angles convention to synthesize an over-constrained PPPRR mechanism. First, five arbitrary angular parameters $\{\theta_{c2}, \theta_{c3}, \alpha_1, \alpha_2, \alpha_3\} = \{-60^\circ, -70^\circ, 50^\circ, 40^\circ, 55^\circ\}$ and seven link parameters $\{d_{c4}, d_{c5}, a_1, a_2, a_3, a_4, a_5\} = \{85, 55, 180, 140, 130, 100, 120\}$ are assumed and substituted into Table III, which is tabulated in Table X.

Next, substituting five arbitrary angular parameters $\{\theta_{c2}, \theta_{c3}, \alpha_1, \alpha_2, \alpha_3\} = \{-60^\circ, -70^\circ, 50^\circ, 40^\circ, 55^\circ\}$ and $\theta_{c1} = 0$ into rotation matrix 0_3R in Eq. (4) yields,

$${}^0_3R(\theta_{c1} = 0, \theta_{c2}, \theta_{c3}, \alpha_1, \alpha_2, \alpha_3) = \begin{bmatrix} a_{11} & a_{12} & a_{13} \\ a_{21} & a_{22} & a_{23} \\ a_{31} & a_{32} & a_{33} \end{bmatrix} \tag{66}$$

Then, use Eq. (A3) to calculate Euler angle β , which is

$$\beta = \pm \cos^{-1} a_{33} = \pm 87.273^\circ \tag{67}$$

Here, the negative value of Euler angle β is adopted to solve for Euler angle γ using Eq. (A5), which are

$$\gamma = \text{atan2}(-a_{13}, a_{23}) = 63.0047^\circ \tag{68}$$

Table XI. D-H table for synthesized PPPRR mechanism.

Link	θ_i	d_i	a_i	α_i
1	-63.0047°	d_1	180	50°
2	-60°	d_2	140	40°
3	-70°	d_3	130	55°
4	θ_4	85	100	0
5	θ_5	55	120	87.273°

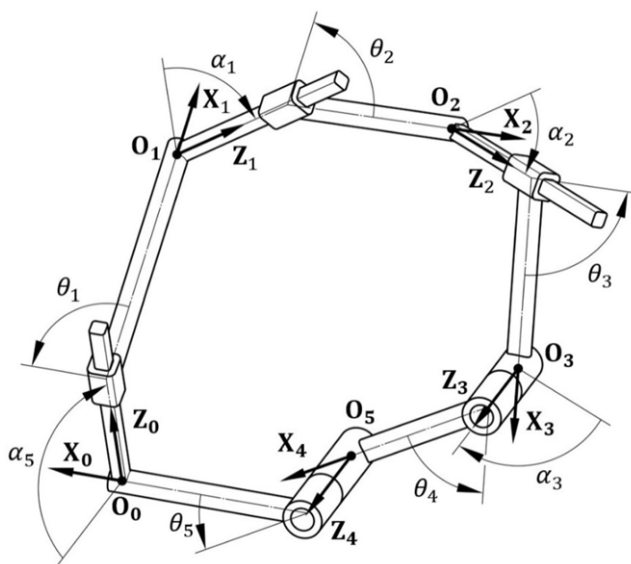


Figure 9. Synthesized PPPRR mechanism using presented methodology.

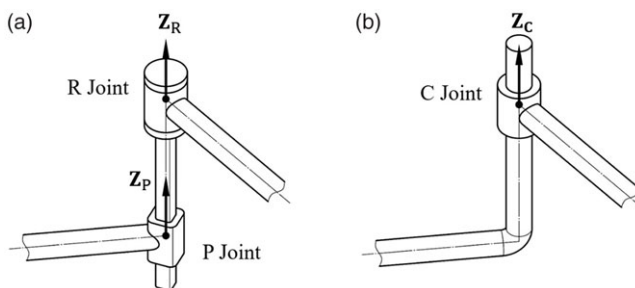


Figure 10. Cylindrical joint formed by a revolute and a prismatic joint along the same axis.

The aforementioned results, which are tabulated in Table XI, can be used to structure a closed-loop PPPRR mechanism, as shown in Fig. 9.

4.2. Isomers of PPPRR mechanism

The cylindrical joint is a joint that provides one translational and one rotational of freedom along the same joint axis. Therefore, when two adjacent R joints and P joints are shown in Fig. 10(a) where the R joint axis Z_R and P joint axis Z_P are coaxial, the R joint and P joint will be configured to a cylindrical joint, as shown in Fig. 10(b).

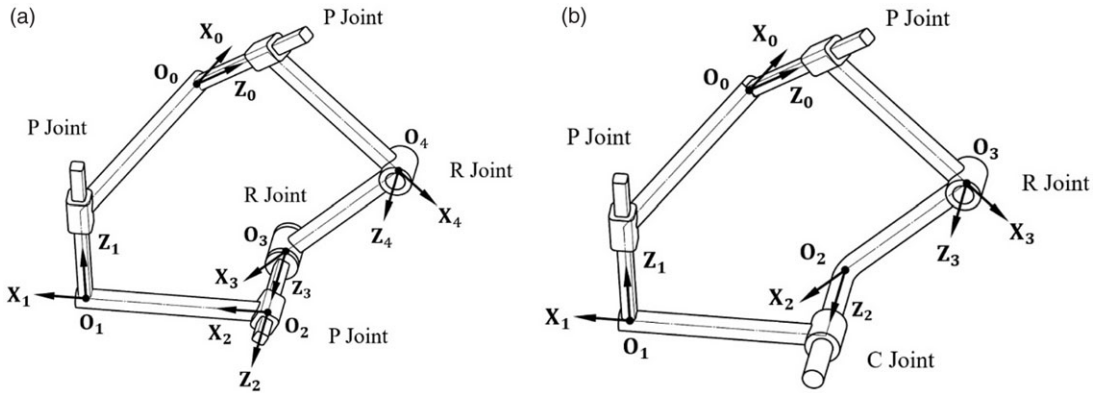


Figure 11. Synthesized PPPRR mechanism and its isomer.

Because of a cylindrical joint that can be formed by a revolute and a prismatic joint along the same axis, the synthesized PPPRR mechanism can be transformed into another over-constrained mechanism with a cylindrical joint. For example, set $a_3 = 0$ and $\alpha_3 = 0$ in Table VIII, a PPPRR mechanism based on the ZXZ Euler angles convention can be synthesized in Fig. 11(a), where P joint axis Z_2 and R joint axis Z_3 and are coaxial. Thus, a PPCR mechanism can be formed, in Fig. 11(b), by combining the P joint and R joint into a cylindrical joint. In addition, the D-H parameters describing the closed-loop equation of the PPCR mechanism can be listed in Table XII.

5. Mobile assemblies derived from PPPRR and PPCR mechanisms

In this section, synthesized PPPRR and PPCR mechanisms can be further used as source modules to form other mobile assemblies. These assemblies may provide a much large archive allowing the engineers to choose desired motions and trajectories. To synthesize new mechanisms configurationally, link parameters of PPPRR and PPCR mechanisms are correspondingly adjusted such that two source modules can be assembled as another over-constrained mechanism.

5.1. RRPRRP mechanism

Figure 12 shows an assembly configuration of the two PPPRR mechanisms and their schematics. In Fig. 12(a), Z_i is the direction of axis i , and $[a_i, \alpha_i]$ represent the common normals and the skew angles between joint axes Z_i and Z_{i+1} . The joint variable of a revolute joint of axis Z_i is denoted by θ_i , while the joint variable of a prismatic joint is denoted by θ_{ci} , a constant value. When the PPPRR mechanism is configured based on the presented method using the ZXZ Euler angles convention, angular parameters $\theta_{c2}, \theta_{c3}, \alpha_1, \alpha_2$, and α_3 can be freely assigned. Hence, $[a_1, \alpha_1]$ of the first PPPRR mechanism can be set equal to $[a_2, \alpha_2]$ of the second PPPRR mechanism. In addition, θ_{c2} of the first PPPRR mechanism can be set equal to $\theta_{c2'}$ of the second PPPRR mechanism. In doing so, Z_1, Z_2 , and Z_3 are, respectively, parallel to Z_1', Z_2' , and Z_3' , as schemed in Fig. 12(b).

Next, combining these PPPRR mechanisms by aligning $[a_1, \alpha_1]$ with $[a_1', \alpha_1']$ and $[a_2, \alpha_2]$ with $[a_2', \alpha_2']$ leads to coincidences of Z_1 and Z_1', Z_2 and $Z_2',$ and Z_3 and Z_3' , as shown in Fig. 12(c).

Now, joint variable d_2 of the first PPPRR mechanism is constrained to be joint variable d_2' of the second PPPRR mechanism. Therefore, two PPPRR mechanisms with independent motion are synchronized. Afterward, collinearly overlapped links $[a_1, \alpha_1]$ and $[a_1', \alpha_1']$ as well as $[a_2, \alpha_2]$ with $[a_2', \alpha_2']$ now can be removed to form a single closed-loop six-bar RRPRRP mechanism in Fig. 13(a). Since the prismatic joints along axis Z_3 and are coaxial, they can be equivalently replaced by one prismatic joint adjacent to link $[a_3, \alpha_3]$ and $[a_3', \alpha_3']$. Besides, the twisted angle of the substitute prismatic joint

Table XII. Link parameters involving ZXZ Euler angles convention for the closed-loop PPCR mechanism.

Link	θ_i	d_i	a_i	α_i
1	$-\gamma$	d_1	a_1	α_1
2	θ_{c2}	d_2	a_2	α_2
3	$\theta_{c3} + \theta_4$	$d_3 + d_{c4}$	a_4	0
4	$-\alpha - \theta_4$	d_{c5}	a_5	$-\beta$

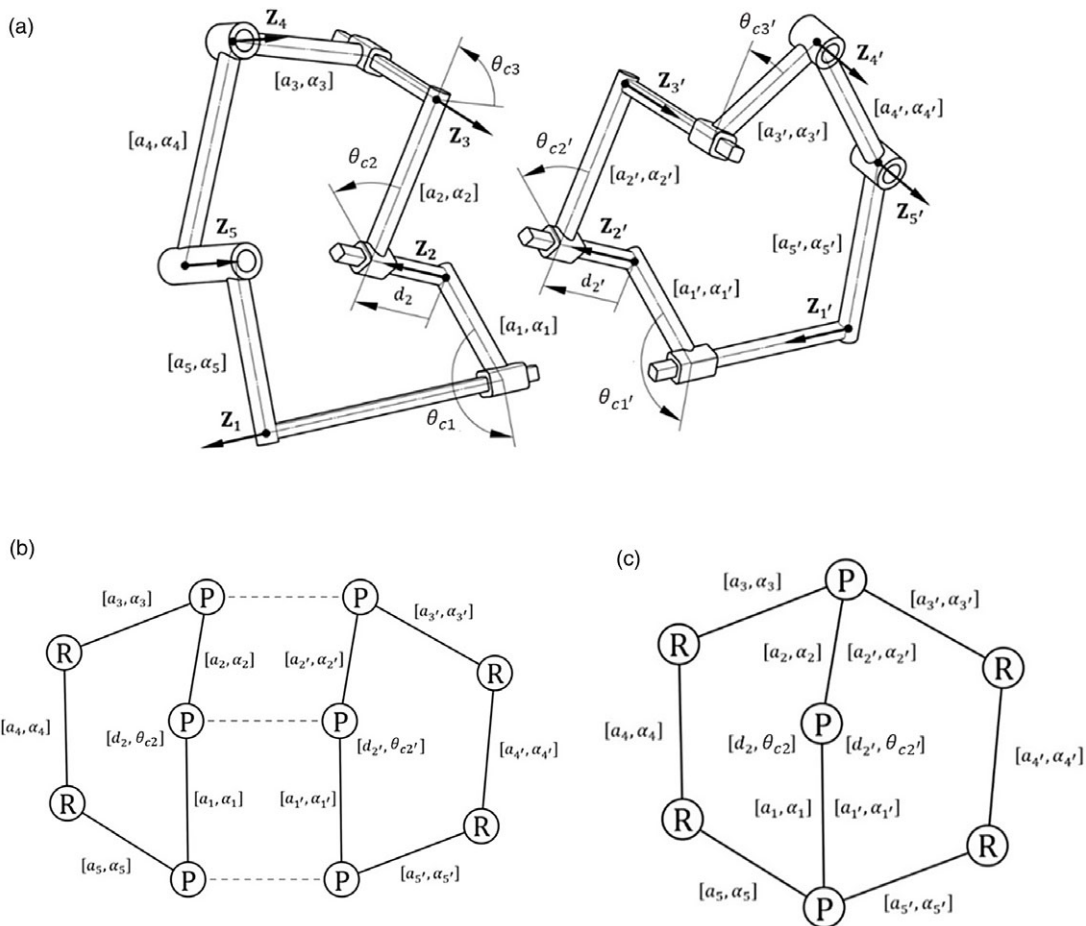


Figure 12. Assembly of the two PPPRR mechanisms and their schematics.

is $\theta_{c3'} - \theta_{c3}$. Likewise, the prismatic joints along axis Z_1 and Z_1' can be equivalently replaced by one prismatic joint adjacent to link $[a_1, \alpha_1]$ and $[a_1', \alpha_1']$. Besides, the twisted angle of the substitute prismatic joint is $\theta_{c1} - \theta_{c1'}$. The rest of $[a_i, \alpha_i]$ for the synthesized RRPRRP mechanism are all identical to these of original PPPRR mechanisms. In addition, due to the constraint $d_2 = d_2'$, the movement of the synthesized RRPRRP mechanism is the same as the two PPPRR mechanisms run synchronously with equal input variables, as simulated in Fig. 13(b).

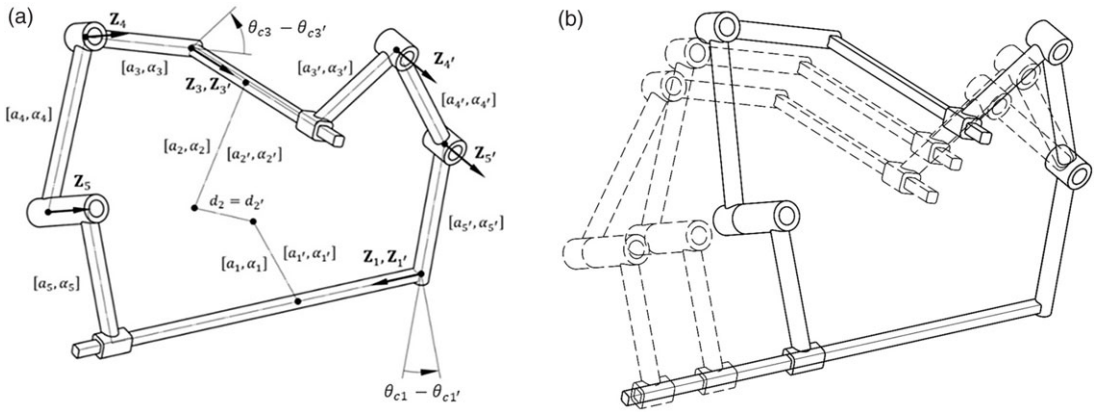


Figure 13. Synthesized RRPRP mechanism and its motion animation.

5.2. RRPRC mechanism

Figure 14(a) shows an assembly configuration of the PPPRR and PPCR mechanism. As mentioned, five angular parameters θ_{c2} , θ_{c3} , α_1 , α_2 , and α_3 of the PPPRR mechanism can be freely assigned. However, for the PPCR mechanism, only three angular parameters θ_{c2} , α_1 , and α_2 can be freely assigned. Hence, $[a_1, \alpha_1]$ and $[a_2, \alpha_2]$ of the PPPRR mechanism can be set equal to $[a_1', \alpha_1']$ and $[a_2', \alpha_2']$ of the PPCR mechanism. In addition, θ_{c2} of the PPPRR mechanism can be set equal to θ_{c2}' of the PPCR mechanism. In doing so, Z_1 , Z_2 , and Z_3 are, respectively, parallel to Z_1' , Z_2' , and Z_3' , as schemed in Fig. 14(b).

Next, aligning $[a_1, \alpha_1]$ with $[a_1', \alpha_1']$ and $[a_2, \alpha_2]$ with $[a_2', \alpha_2']$ yield coincidences of Z_1 and Z_1' , Z_2 and Z_2' , and Z_3 and Z_3' , as shown in Fig. 14(c). Now, joint variable d_2 of the PPPRR mechanism is constrained to be joint variable d_2' of the PPCR mechanism. Therefore, two mechanisms with independent motion are synchronized. Afterward, removing collinearly overlapped links $[a_1, \alpha_1]$ and $[a_1', \alpha_1']$ as well as $[a_2, \alpha_2]$ with $[a_2', \alpha_2']$ yields a single closed-loop five bar RRPRC loop in Fig. 15(a). In the combined loop, the prismatic joint along axis Z_3 and the cylindrical joint along Z_3' are coaxial, they can be equivalently replaced by one cylindrical joint adjacent to link $[a_3, \alpha_3]$ and $[a_3', \alpha_3']$. Besides, the twisted angle of the substitute prismatic joint is $\theta_{c3}' - \theta_{c3}$. Likewise, the prismatic joints along axis, Z_1 and Z_1' can be equivalently replaced by one prismatic joint adjacent to link $[a_1, \alpha_1]$ and $[a_1', \alpha_1']$. Besides, the twisted angle of the substitute prismatic joint is $\theta_{c1} - \theta_{c1}'$. The rest of $[a_i, \alpha_i]$ for the synthesized RRPRC mechanism are all identical to these of original PPPRR and PPCR mechanisms. The synthesized RRPRC mechanism should be immobile since its mobility is zero based on the prediction of Chebychev–Grübler–Kutzbach criterion. However, its mobility inherit from the synchronized motion of input variables $d_2 = d_2'$ driving the combined PPPRR and PPCR mechanism, as simulated in Fig. 15(b).

5.3. RCRC mechanism

By the same token, two PPCR mechanisms are assembled as shown in Fig. 16(a) and schematized in Fig. 16(b). Three angular parameters θ_{c2} , α_1 , and α_2 for these two PPCR mechanisms can be correspondingly assigned such that $[a_1, \alpha_1]$ and $[a_2, \alpha_2]$ of the first PPCR mechanism are equal to $[a_1', \alpha_1']$ and $[a_2', \alpha_2']$ of the second PPCR mechanism. In addition, θ_{c2} of the first PPCR mechanism can be set equal to $-\theta_{c2}'$ of the second PPCR mechanism such that Z_1 , Z_2 , and Z_3 are, respectively, parallel to Z_3' , Z_2' , and Z_1' , as schemed in Fig. 16(b).

Next, two PPCR mechanisms can be combined by aligning $[a_1, \alpha_1]$ with $[a_1', \alpha_1']$ and $[a_2, \alpha_2]$ with $[a_2', \alpha_2']$ so as to achieve coincidences of Z_3 and Z_1' , Z_2 and Z_2' , and Z_1 and Z_3' , as shown in Fig. 16(c). Now, two PPCR mechanisms move synchronously with equal input variables due to the constraint

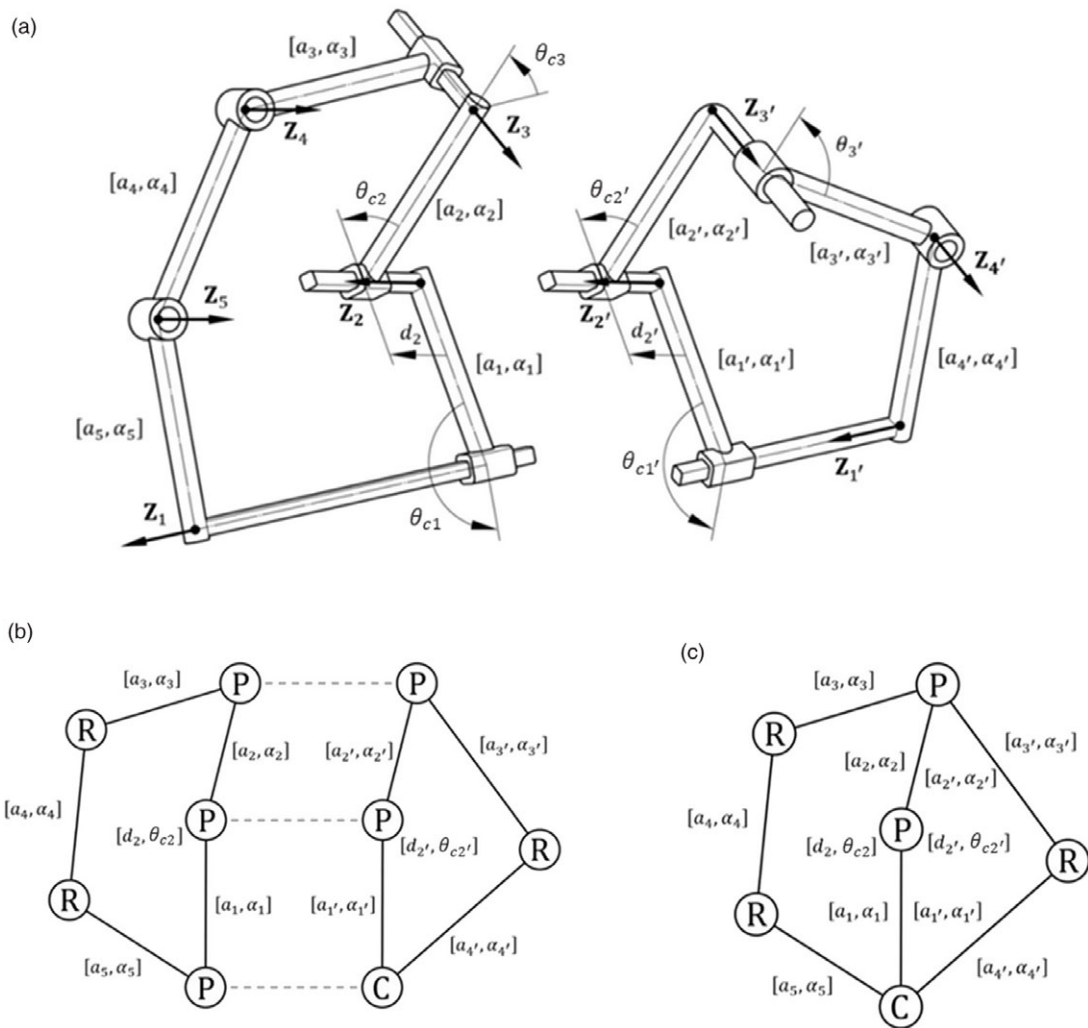


Figure 14. Assembly of the PPPRR and PPCR mechanisms and their schematics.

$d_2 = d_2'$. Afterward, a single closed-loop four-bar RCRC loop in Fig. 17(a) can be formed by removing collinearly overlapped links $[a_1, \alpha_1]$ and $[a_2, \alpha_2]$ as well as $[a_2, \alpha_2]$ with $[a_1', \alpha_1']$. In the combined loop, the prismatic joint along axis Z_1 and the cylindrical joint along Z_3 can be equivalently substituted by a cylindrical joint adjacent to link $[a_1, \alpha_1]$ and $[a_3, \alpha_3]$. Besides, the twisted angle of the substitute cylindrical joint is $\theta_{c1} + \theta_3$. Likewise, the prismatic joints along axis Z_3 and Z_1' can be equivalently substituted by a cylindrical joint adjacent to link $[a_3, \alpha_3]$ and $[a_1', \alpha_1']$. Besides, the twisted angle of the substitute prismatic joint is $\theta_3 + \theta_{c1}'$. The rest of $[a_i, \alpha_i]$ for the synthesized RCRC mechanism are all identical to these of original PPCR mechanisms. The synthesized RCRC loop is also an over-constrained mechanism, as simulated in Fig. 17(b). An intriguing research that relates the RCRC linkage and its resemble linkage, the RCCC linkage, is the passive coupling method proposed by Dimentberg [23]. He suggests synthesizing the RCRC linkage by locking the degree of freedom of one revolute joint of the RCCC linkage. This approach may provide an extended investigation of the ongoing discussion but is not within the scope of this paper.

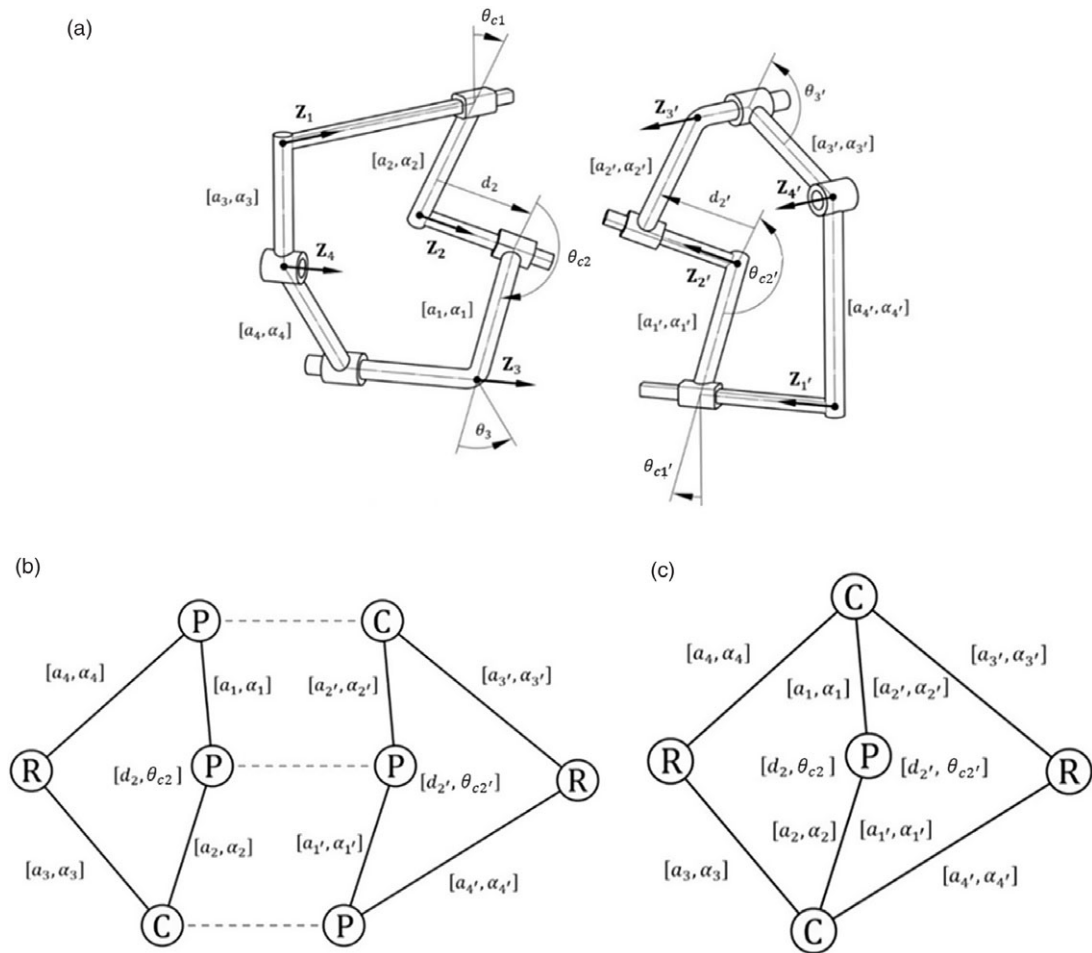


Figure 16. Assembly of two PPCR mechanisms and their schematics.

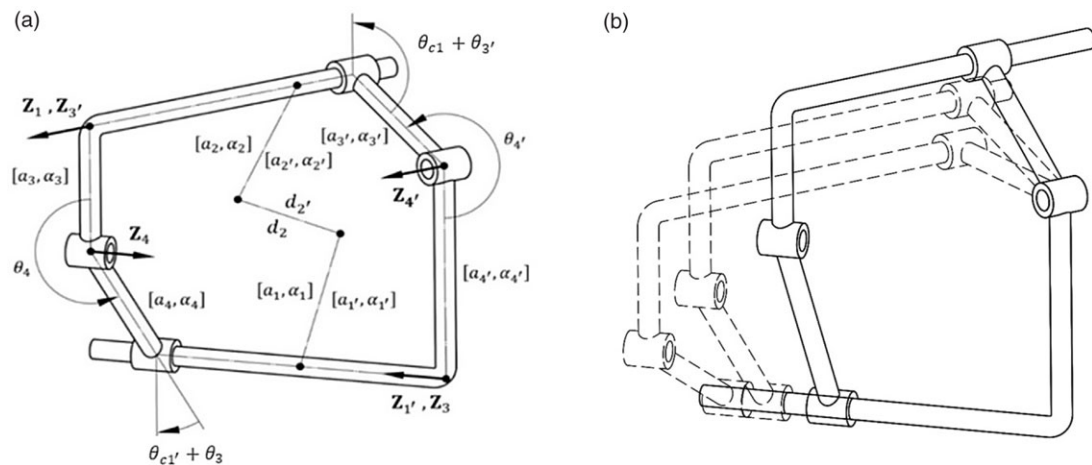


Figure 17. Synthesized RCRC mechanism and its motion animation.

geometrical constraints from closed-loop equation analytically, the modular method presented in this research is more intuitive to find the over-constrained mechanisms.

In addition, our work aims to provide a synthesis method of spatial over-constrained mechanisms based on the kinematics of a specific serial manipulator. Some concepts are similar to the previous studies by Li and Angeles's work [25, 26]. They are devoted to promote a 3-CCC parallel manipulator by refining its kinematic, singularity, workspace, and dexterity analyses. To the goal for both of our research, kinematic analyses that describe the input/output function among mating parts are required. One noticeable difference between our methods is the mathematical foundations adopted. We apply D-H notations to relate link dimensions and joint variables for the serial manipulator and derive the position and orientation of the manipulator end-effector based on the homogeneous transformation matrix representation. Li and Angeles's work establishes the constraint-screw systems for every CCC limb [25] and solves a quartic resolvent polynomial to yield the orientation of the moving platform. Although the mathematical formulations are distinct, both of our works attempt to simplify the analyses by decoupling the rotational and translational motion of the end-effector. We verify that the serial PPP manipulator has an unchanged orientation and unlimited workspace by separately examining the elements governing rotation and translation. Hence, we can concentrate on aligning the orientations of the end-effector coordinate system of two manipulators without paying attention to coinciding the origin of the end-effector coordinate system. Li and Angeles reveal that the orientation of 3-CCC PKM can be individually solved without considering the linear displacement of the cylindrical joints. Besides, they found that the singularity of the 3-CCC PKM only results from the orientation of the moving platform. Both of our works indicate that the complexity of a kinematic problem may be reduced by considering the rotation and translation of the links individually. This feature, as suggested by Li and Angeles [25, 26], may provide an intriguing enlightenment on relevant research in the future.

Acknowledgments. The authors also wish to acknowledge the support of the Department of Mechanical Engineering at National Taiwan University. In addition, the corresponding author offers his grateful thanks to the dedicated referees of this work, whose collective comments form the fundamentals of the research. Most importantly, the Young Scholar Fellowship Program, supported by the Ministry of Science and Technology of Taiwan, encourages the corresponding author to fearlessly devote to his research.

Conflicts of interest. The authors declare no conflict of interest.

Financial support. This work was supported by the Ministry of Science and Technology of Taiwan (MOST 110-2636-E-002-023 and MOST 111-2222-E-002-002-MY3).

Ethical considerations. None.

Authors' contributions. All authors contributed to the study conception and design. Material preparation, data collection, and analysis were performed by Fu-Hsiung Lee. The first draft of the manuscript was written by Kuan-Lun Hsu, and all authors commented on previous versions of the manuscript. All authors read and approved the final manuscript.

References

- [1] G. M. Grübler. *Getriebelehre: eine Theorie des Zwanglaufes und der ebenen Mechanismen* (Springer, Germany, 1917).
- [2] K. Kutzbach, "Mechanische leitungsverzweigung, ihre gesetze und anwendungen," *Maschinenbau* **8**(21), 710–716 (1929).
- [3] G. T. Bennett, "A new mechanism," *Engineering* **76**, 777–778 (1903).
- [4] E. Delassus, "Sur les systèmes articulés gauches, Première partie," *Ann. Sci. 3s* Vol **17**, 455–499 (1900).
- [5] E. Delassus, "Sur les systèmes articulés gauches, deuxième partie," *Ann. Sci. 3s* Vol **19**, 119–152 (1902).
- [6] E. Delassus, "Les chaînes articulées fermées et déformables à quatre membres," *Bull. Sci. Math.* **46**(2), 283–304 (1922).
- [7] F. M. Dimentberg and I. V. Yoslovich, "A spatial four-link mechanism having two prismatic pairs," *J. Mech.* **1**(3–4), 291–300 (1966).
- [8] M. Savage, "Four-link mechanisms with cylindrical, revolute and prismatic pairs," *Mech. Mach. Theory* **7**(2), 191–208 (1972).
- [9] K. H. Hunt, "Prismatic pairs in spatial linkages," *J. Mech.* **2**(2), 213–216, in7-in8, 217–230 (1967).
- [10] K. J. Waldron, "A study of overconstrained linkage geometry by solution of closure equations - Part II. Four-bar linkages with lower pair joints other than screw joints," *Mech. Mach. Theory* **8**(2), 233–247 (1973).

[11] K. J. Waldron, "A study of overconstrained linkage geometry by solution of closure equations - Part I. Method of study," *Mech. Mach. Theory* **8**(1), 95–104 (1973).

[12] P. R. Pamidi, "Existence criteria of overconstrained mechanisms with two passive couplings," Ph.D., Faculty of the Graduate College of Oklahoma State University (1970).

[13] P. R. Pamidi and A. H. Soni, "Necessary and sufficient existence criteria of overconstrained Five-Link spatial mechanisms with helical, cylinder, revolute, and prism pairs," *J. Eng. Ind.* **95**(3), 737–743 (1973).

[14] J. E. Baker, "Overconstrained 5-bars with parallel adjacent joint axes — I method of analysis," *Mech. Mach. Theory* **13**(2), 213–218 (1978).

[15] J. E. Baker, "Overconstrained 5-bars with parallel adjacent joint axes—II the linkages," *Mech. Mach. Theory* **13**(2), 219–233 (1978).

[16] C.-C. Lee and J. Hervé, "Synthesize New 5-Bar Paradoxical Chains Via the Oblique Circular Cylinder," In: *Mechanism and Machine Theory - MECH MACH THEOR.* vol. **46** (2011) pp. 784–793.

[17] S. Guo, H. Qu, Y. Fang and C. Wang, "The dof degeneration characteristics of closed loop overconstrained mechanisms," *Trans. Can. Soc. Mech. Eng.* **36**(1), 67–82 (2012).

[18] M. Goldberg, "New five-bar and six-bar linkages in three dimensions," *Trans. ASME* **65**, 649–661 (1943).

[19] K. J. Waldron, "Hybrid overconstrained linkages," *J Mech.* **3**(2), 73–78 (1968).

[20] J. E. Baker, "A comparative survey of the Bennett-based, 6-revolute kinematic loops," *Mech. Mach. Theory* **28**(1), 83–96 (1993).

[21] Y. Chen, "An extended myard linkage and its Derived 6R linkage," *J. Mech. Design* **130**(5), 777 (2008).

[22] J. Denavit and R. S. Hartenberg, "A kinematic notation for Lower-Pair mechanisms based on matrices," *J. Appl. Mech.* **22**(2), 215–221 (1955).

[23] F. M. Dimentberg, "A general method for the investigation of finite displacement of spatial mechanisms and certain cases of passive constraints," *Proc. Sem. Theory Mach. Mech. Acad. Sci. USSR* **5**(17), 5–39 (1948).

[24] K. Wohlhart, "Merging two general Goldberg 5R linkages to obtain a new 6R space mechanism," *Mech. Mach. Theory* **26**(7), 659–668 (1991).

[25] W. Li and J. Angeles, "Full-mobility three-CCC parallel-kinematics machines kinematics and isotropic design," *ASME J. Mech. Robot.* **10**(1), 011011 (2018).

[26] W. Li and J. Angeles, "Full-mobility 3-CCC parallel-kinematics machines: forward kinematics, singularity, workspace and dexterity analyses," *Mech. Mach. Theory* **126**, 312–332 (2018).

[27] T. Yoshikawa. *Foundations of Robotics: Analysis and Control* (MIT Press, USA, 1990).

[28] R. N. Jazar. *Theory of Applied Robotics: Kinematics, Dynamics, and Control* (Springer Science & Business Media, Germany, 2010).

Appendix A

Euler Angle Representation for Rotation Matrices

The orientation of the PPP manipulator can be defined by the Euler angle representation [27,28]. Hence, this section summarizes the conventions of ZXZ Euler angles and XZX Euler angles, respectively. First, to describe the orientation of the end-effector coordinate system $O_3X_3Y_3Z_3$ using the ZXZ Euler angles convention, all elements of rotation matrix 0_3R are set to be equal to these of rotation operator $R_z(\gamma) R_x(\beta) R_z(\alpha)$ specified by ZXZ Euler angles (α, β, γ) , which can be expressed as

$${}^0_3R = R_z(\gamma) R_x(\beta) R_z(\alpha) \tag{A1}$$

namely,

$$\begin{bmatrix} a_{11} & a_{12} & a_{13} \\ a_{21} & a_{22} & a_{23} \\ a_{31} & a_{32} & a_{33} \end{bmatrix} = \begin{bmatrix} c\alpha c\gamma - s\alpha c\beta s\gamma & -c\gamma s\alpha - c\alpha c\beta s\gamma & s\beta s\gamma \\ s\alpha c\beta c\gamma + c\alpha s\gamma & c\alpha c\beta c\gamma - s\alpha s\gamma & -s\beta c\gamma \\ s\alpha s\beta & c\alpha s\beta & c\beta \end{bmatrix} \tag{A2}$$

Analyzing Eq. (A2) allows to find the solution of the required ZXZ Euler angles (α, β, γ) , which can be expressed as

$$\beta = \pm \cos^{-1} a_{33} \tag{A3}$$

$$\alpha = \text{atan2}(\pm a_{31}, \pm a_{32}) \tag{A4}$$

$$\gamma = \text{atan2}(\pm a_{13}, \mp a_{23}) \tag{A5}$$

Similarly, to describe the orientation of the end-effector coordinate system $O_3X_3Y_3Z_3$ using the XZX Euler angles convention, all elements of rotation matrix 0_3R are set to be equal to these of rotation operator $R_x(\gamma) R_z(\beta) R_x(\alpha)$ specified by XZX Euler angles (α, β, γ) , which can be expressed as

$${}^0_3R = R_x(\gamma) R_z(\beta) R_x(\alpha) \tag{A6}$$

namely,

$$\begin{bmatrix} a_{11} & a_{12} & a_{13} \\ a_{21} & a_{22} & a_{23} \\ a_{31} & a_{32} & a_{33} \end{bmatrix} = \begin{bmatrix} c\beta & -c\alpha s\beta & s\alpha s\beta \\ s\beta c\gamma & c\alpha c\beta c\gamma - s\alpha s\gamma & -s\alpha c\beta c\gamma - c\alpha s\gamma \\ s\beta s\gamma & s\alpha c\gamma + c\alpha c\beta s\gamma & c\alpha c\gamma - s\alpha c\beta s\gamma \end{bmatrix} \tag{A7}$$

Analyzing Eq. (A7) allows to find the solution of the required XZX Euler angles (α, β, γ) , which can be expressed as

$$\beta = \pm \cos^{-1} a_{11} \tag{A8}$$

$$\alpha = \text{atan2}(a_{13}, -a_{12}) \tag{A9}$$

$$\gamma = \text{atan2}(a_{31}, a_{21}) \tag{A10}$$